

## Lyman- $\alpha$ emission from proton bombardment of Si, Cu, Ge, Mo, Ta, and Pt surfaces

Yu-Yuan R. Hsiao and Robert C. Amme

Department of Physics, University of Denver, Denver, Colorado 80208

(Received 7 November 1978)

A 0.3-m vacuum monochromator has been used to observe Lyman- $\alpha$  emission from polycrystalline Mo, Ta, Pt, and Cu and from single-crystal  $n$ -type Ge and Si surfaces under 6.5–12.5-keV proton bombardment. The viewing direction was fixed at  $60^\circ$  relative to the proton-beam axis. The absolute photon yields were determined as a function of beam-surface incidence angle ( $\theta = 0$  for normal incidence) and surface temperature (300–600 °K). Yields exhibited incident angle dependences of  $\sec\theta$  or stronger, and temperature coefficients were positive for Mo and Ta, negative for Cu, and nearly zero for Ge. Doppler-shift profiles of the Lyman- $\alpha$  emission were used to determine the backscattered, excited-hydrogen-atom energies. Absolute photon yields between about  $10^{-4}$  and  $10^{-2}$  photons/proton were obtained. The yields were insensitive to background  $H_2$  gas pressure between  $5 \times 10^{-9}$  and  $10^{-7}$  Torr.

### I. INTRODUCTION

The emission of Lyman- $\alpha$  ( $L_\alpha$ ) radiation from proton bombardment of surfaces was first reported by Dunn, Geballe, and Pretzer<sup>1</sup> in 1962.  $L_\alpha$  emission was observed from tungsten mesh under impact by 2.5-keV protons with a photon yield of  $5 \times 10^{-3}$  photon/proton. In 1966, Sterk, Mark, and Saylor<sup>2</sup> bombarded an aluminum surface oriented at  $30^\circ$  with respect to a proton beam. Their proton energy was varied from 3 to 30 keV. The results of this experiment agreed closely with those of Dunn *et al.* In 1967, Khan, Potter, Worley, Salem, and Smith<sup>3</sup> investigated  $L_\alpha$  emission from a single crystal of copper. Here, the crystal was exposed alternately to beams of protons and helium ions and the emission spectrum from the surface was observed. No absolute calibration was attempted, however.

McCracken and Erents,<sup>4</sup> in 1970, observed  $L_\alpha$  emission by bombarding a Mo surface with  $H^+$ ,  $H_2^+$ , and  $H_3^+$  ions of energies ranging from 12 to 33 keV. They measured the  $L_\alpha$  line profiles, which showed Doppler shift and broadening. In other work<sup>5</sup> they indicated that the  $L_\alpha$  photon yield from Mo surfaces is of the order of  $10^{-4}$  photon/proton when 20-keV ions are incident at  $45^\circ$  with respect to the surface normal. Note that this yield is more than an order of magnitude below that reported by Dunn *et al.*

In view of these relatively few published results on  $L_\alpha$  emission from surfaces and the considerable difference between observations, additional study is warranted. The purposes of the research reported here have been to determine absolute photon yields for a wider variety of surface materials, to determine the dependence of the yield on incident proton angle and energy, and to observe the temperature dependence of the yield. These re-

sults, coupled with data by other investigators on observed Balmer emissions,<sup>6–9</sup> should provide insight into the mechanisms of surface scattering and neutralization.

### II. EXPERIMENTAL DETAILS

A schematic diagram of the apparatus is presented in Fig. 1. The protons are generated in an rf discharge ion source,<sup>10</sup> and are accelerated to the desired energy before entering a magnetic

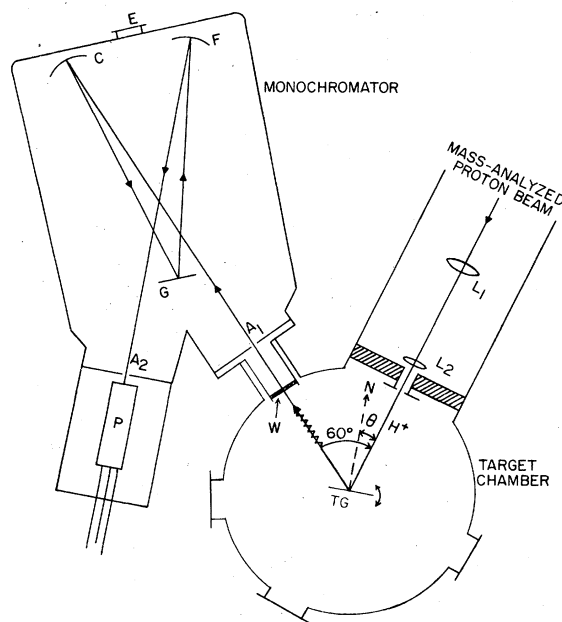


FIG. 1. Schematic diagram of the apparatus. TG is the target surface which can be rotated about the vertical axis.  $\theta$  is the beam incident angle and is measured from the target normal  $N$ .  $W$  is a polished LiF window of 1 mm thickness.

mass analyzer. When the beam emerges from the mass analyzer it is collimated by two electrostatic lenses ( $L_1$  and  $L_2$ ) before entering the scattering chamber. Inside the scattering chamber are two restricting apertures to limit the beam size to about 2.5 mm in diameter and  $4^\circ$  angular divergence. The proton energy can be adjusted between 6.5 and 12.5 keV with an energy spread of about 200 eV full width at half maximum. The target can be rotated through  $360^\circ$  around a vertical axis passing through the target surface and perpendicular to the beam direction, and can also be displaced vertically by 2.5 cm. The incident angle  $\theta$  is measured with respect to the surface normal.

The observed radiation passes through a 0.3-m,  $f/5.6$ , McPherson model-218 vacuum monochromator and is detected by an EMR Model 541F-08-18-03900 photomultiplier operating in a pulse counting mode. The monochromator is fixed at a position which makes an angle of  $60^\circ$  with respect to the ion-beam direction, and in a plane containing the target surface normal and the beam direction. It is fitted with a 600-line/mm  $\text{MgF}_2$ -coated plane grating  $G$  blazed at  $1500 \text{ \AA}$ , and is capable of viewing the whole area of the target surface.

The pressure within the scattering chamber during bombardment is maintained at  $1-5 \times 10^{-8}$  Torr by two Electroion pumps in a differential pumping arrangement. The scattering chamber and monochromator are separated by a 1-mm-thick LiF window ( $W$ ).

Not shown in Fig. 1 is a deep Faraday cup which is attached to the rear of the target mount. The cup, fitted with a grid for secondary electron suppression, is used to measure the proton-beam intensity. A typical beam current is about  $25 \mu\text{A}$ , giving a current density of about  $500 \mu\text{A}/\text{cm}^2$ . With the target in position, only the apparent beam current to the target may be monitored. This apparent current depends strongly on the secondary-electron-emission coefficient, which in turn depends on the energy of the proton beam, the incident angle, and the surface condition of the target. Therefore, it provides only an indication of the constancy of the incident beam current during a given measurement.

The Cu, Mo, Ta, and Ge target surfaces were mechanically polished with 1- $\mu\text{m}$  diamond dust using kerosene as vehicle. The polished surfaces are rinsed with deionized water, acetone, and trichloroethylene, in that order. The Cu, Mo, and Ta targets are polycrystalline bulk material, but the Pt surface is a foil of 0.04 mm thickness. The photon yield has been measured from both  $n$ -type and pure Si, which are supplied as polished wafers from Motorola Company. The Ge and Si surfaces are the (111) face, as determined by x-ray diffrac-

tion. The Ge is doped  $n$ -type.

The surfaces have been examined by x-ray fluorescence techniques. Traces of Rh and Pd were observed in the Pt sample, traces of Fe, Cu, and W in Mo, and no noticeable trace of impurities in the Cu and Ta targets. For the  $n$ -type Ge a very small amount of As was observed, but for the  $n$ -type Si, no noticeable impurities of elements heavier than Ca were found. However, for the pure Si, some traces of Fe, Cr, and Zn were observed. All of these trace impurities were present in amounts less than 100 ppm and thus probably had minimal influence on the observed  $L_\alpha$  emission yields.

### III. OPTICAL CALIBRATION

In order to determine the absolute  $L_\alpha$  photon yield, it is necessary to determine the overall system efficiency  $\epsilon$ , which depends upon the solid angle subtended by the entrance slit from the target and the efficiencies of the monochromator and photomultiplier. To determine these quantities individually is a formidable task. Instead, a "standard source" was constructed (Fig. 2) that is used to calibrate the  $L_\alpha$  spectral line position of the monochromator as well as to determine  $\epsilon$  experimentally. The calibration assembly is similar to that employed by Mumma and Zipf<sup>11</sup> in their investigation of electron impact on gases. It con-

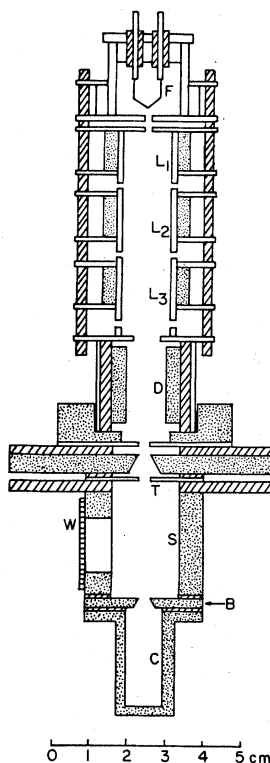


FIG. 2. Standard  $L_\alpha$  source assembly.  $F$  is the electron gun filament,  $L_1$ ,  $L_2$ , and  $L_3$  are electron collimation lenses,  $D$  is the electron beam deflector,  $T$  is the top plate of the scattering cell,  $S$  is the cell wall,  $B$  is the cell bottom plate,  $C$  is the Faraday cup, and  $W$  is the LiF window.

tains an electron gun and a cylindrical cell at known pressure of  $H_2$  gas. The electrons are magnetically shielded so that a well-collimated beam may pass through the center of the scattering cell. The entire assembly is mounted on a flange identical to that from which the target is suspended. The target assembly may be removed from the scattering chamber and the calibration assembly may be placed in the same position as the target surface. The cell is provided with a LiF window 15.2 mm long and 1 mm thick. The electron current is monitored separately to the cell top  $I_T$ , the cell wall  $I_S$ , the cell bottom plate  $I_B$ , and the Faraday cup  $I_C$ . Typical current measurements are as follows:  $I_T = 3 \mu A$ ,  $I_S = 2 \mu A$ ,  $I_B = 1.4 \mu A$ , and  $I_C = 39 \mu A$ . Because the current collected by the top plate will not make any significant contribution to the observed photon emission, we disregarded this component. However, the current collected by the cell wall may make some contribution to the photon emission. Because the cell length is 3.0 cm long and the viewing beam length is about half of this, we estimate that about one-half of the electrons collected by the cell wall effectively contribute to the photon emission observed. Since we have a wide open observation window, we expect that those electrons collected by the cell bottom plate should have the same effect as those collected by the Faraday cup as they pass the observation region. From the above discussions we use as the effective electron-beam current

$$I_e = I_C + I_B + \frac{1}{2}I_S. \quad (1)$$

Because of the difficulty of ascertaining the contribution due to  $I_S$ , we impose an uncertainty of  $\pm 15\%$ .

The number of  $L_\alpha$  photons emitted per unit time from electron-beam impact on the  $H_2$  target gas can be expressed as follows:

$$G_L = N_T l \sigma_L B, \quad (2)$$

where  $N_T$  is the scattering cell gas density at temperature  $T$ ,  $\sigma_L$  is the known dissociative cross section for  $L_\alpha$  emission by electron impact on hydrogen,<sup>11,12</sup>  $l$  is the length of the electron beam viewed by the monochromator, and  $B$  is the electron-beam flux. The rate at which photons are detected by the optical system is

$$S_c = (\epsilon/F)G_L T'_w \quad (3)$$

where  $T'_w$  is the transmission of the scattering cell window and  $F$  is a correction factor due to the presence of molecular uv emission from hydrogen. From the known slit function and the spectral scan reported by Vroom and DeHeer,<sup>12</sup> the results of Stone and Zipf,<sup>13</sup> and McConkey and Donaldson,<sup>14</sup> we estimate the contribution of the molecular line

in this work to about 5%, i.e., the correction factor is given by

$$F = 0.95 \pm 0.05. \quad (4)$$

The number density  $N_T$  at 300 °K is taken from the ideal-gas relationship  $N_T = 3.22 \times 10^{16} P$  ( $cm^{-3}$ ), in which  $P$  is the pressure in Torr.

Combining Eqs. (2), (3), and (4), and setting  $B = 6.25 \times 10^{-12} I_e$  gives

$$\epsilon = 4.72 \times 10^{-30} (S_c / T'_w P \sigma_L I_e l), \quad (5)$$

with  $l$  in cm,  $\sigma_L$  in  $cm^2$ , and  $S_c$  in counts/sec.

The transmission of the LiF window,  $T'_w$ , can be estimated from the known index of refraction,<sup>15</sup> and the published transmittance,<sup>16</sup> of LiF at different thicknesses. Our result for the 1-mm-thick window is

$$T'_w = 0.74 \pm 0.04. \quad (6)$$

Using this value in Eq. (5), along with  $l = 1.52$  cm, gives

$$\epsilon = 4.20 \times 10^{-30} (S_c / P \sigma_L I_e). \quad (7)$$

The cell pressure was monitored by an ionization gauge calibrated for  $H_2$  and was varied from  $10^{-4}$  to  $10^{-3}$  Torr. The electron-beam current was varied from 35 to 55  $\mu A$  at different beam energies. By measuring the counting rate and using the known dissociative excitation cross sections given by Mumma and Zipf,<sup>11</sup> we obtain the optical efficiency of the system:

$$\epsilon = 3.24 \times 10^{-10}. \quad (8)$$

Uncertainties are discussed in Sec. V.

The absolute photon yield at any orientation of the target surface is thus given by

$$Y(\theta) = S(\theta) / B_p \epsilon, \quad (9)$$

where  $S(\theta)$  is the measured counting rate at incident angle  $\theta$  and  $B_p$  is the proton-beam flux. Combining Eqs. (8) and (9) gives

$$Y(\theta) = 4.93 \times 10^{-4} S(\theta) / I \quad (10)$$

with the proton-beam current  $I$  in  $\mu A$ .

#### IV. YIELD MEASUREMENTS

Ultraviolet emission from the surfaces has also been investigated with the monochromator from 1090 to 1330 Å employing 200- $\mu m$  entrance and exit slit widths in an effort to detect any emission other than  $L_\alpha$  in this region. No emission in this interval except the  $L_\alpha$  line was detected with this system. (We have observed Lyman- $\beta$  at 1025 Å, using a channel electron multiplier, without the LiF window inserted between monochromator and scattering chamber).

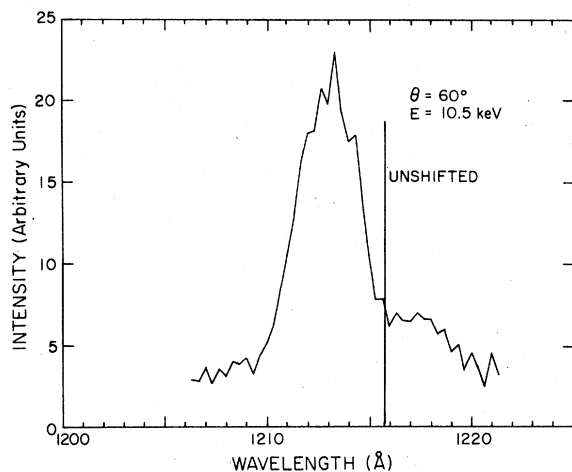


FIG. 3. Line profile of  $L_{\alpha}$  emission from a Cu surface. The unshifted line is 1215.7 Å.

A typical spectral scan of the  $L_{\alpha}$  line from a copper surface bombarded with 10.5-keV protons at a  $60^{\circ}$  angle is shown in Fig. 3. A slit width of  $20 \mu\text{m}$  was employed. The proton energy dependence of the  $L_{\alpha}$  emission is shown in Fig. 4. The temperature of the target was nominally at  $320^{\circ}\text{K}$  and the incident angle of the proton beam was set at  $60^{\circ}$ . Figure 5 shows the dependence of the  $L_{\alpha}$  emission on incident angle for the various target materials. It is important to note that the sample used for measurement on platinum was a thin foil, rather than bulk material. Because of irregularities in the foil surface, the reproducibility is somewhat questionable. Figure 6 shows the dependence of the reduced photon yield,  $Y(\theta)/Y(0)$ , as a function of incident angle, where  $Y(\theta)$  represents the photon yield at angle  $\theta$  and  $Y(0)$  as the photon yield at  $\theta=0$  (normal incidence). Figure 7 shows

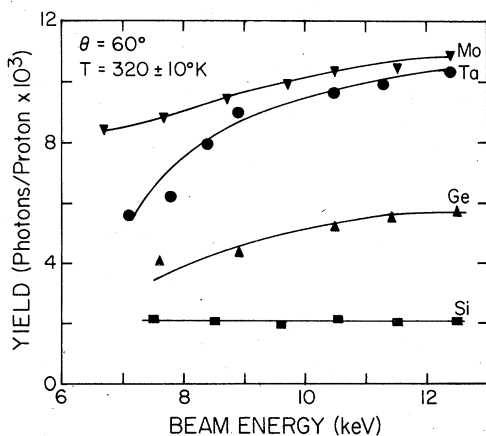


FIG. 4. Energy dependence of the  $L_{\alpha}$  photon yield. Surface temperature is  $320^{\circ}\text{K}$ .

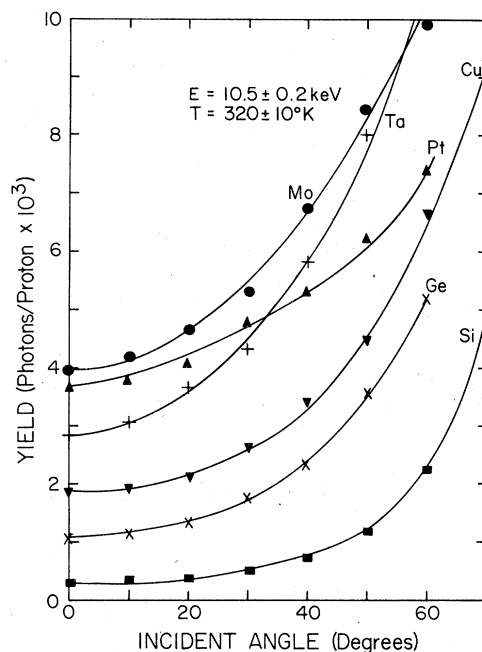


FIG. 5. Angular dependence of the  $L_{\alpha}$  photon yield.

the  $L_{\alpha}$  photon yield at different target temperatures, for an incident angle  $\theta=60^{\circ}$  and 10.5-keV proton energy. Figure 8 shows the photon yields plotted as a function of the target atomic number with a 10.5-keV proton energy. A  $60^{\circ}$  angle of incidence was employed, and the target temperature was maintained around  $320^{\circ}\text{K}$ .

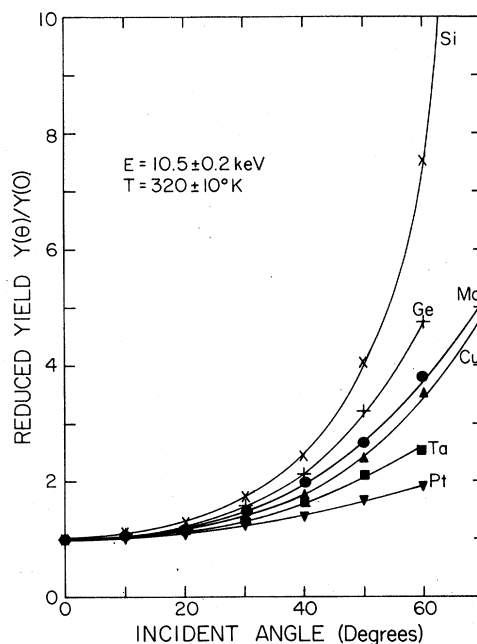


FIG. 6. Angular dependence of the  $L_{\alpha}$  photon yield, reduced to unity at normal incidence.

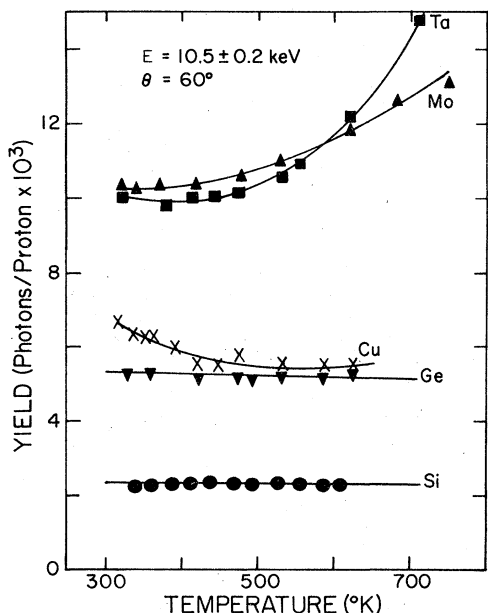


FIG. 7. Observed photon yield as a function of surface temperature.

## V. DISCUSSION

### A. Estimate of uncertainty in yield

The accuracy of the  $L_{\alpha}$  photon-yield measurements depends on the accuracy of the optical calibration, the counting statistics, and the measurement of the proton-beam intensity. By estimating the uncertainties in those quantities on the right-hand side of Eq. (5) we conclude that the uncertainty  $R_{\epsilon}$  of the optical calibration is

$$R_{\epsilon} = \pm 25\%.$$

Also from the statistics of our measurement of

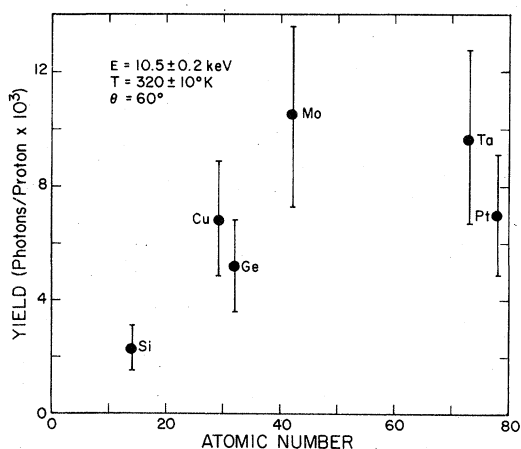


FIG. 8. Photon yield vs atomic number of the target. Error bars represent 25% uncertainty value, due primarily to calibration and counting statistics.

$S(\theta)$  and  $B_p$ , we find that the uncertainty in the ratio  $S(\theta)/B_p$  is  $R_s = \pm 10\%$ . Therefore, we conclude that the uncertainty in the photon yield is

$$R = \pm (R_{\epsilon}^2 + R_s^2)^{1/2} = \pm 27\%. \quad (11)$$

### B. Comparison with previous investigators

From the plot of photon yield as a function of target atomic number, we find that our interpolated result for Al will agree favorably with the result of Sterk *et al.*<sup>2</sup> The atomic number of Ta is 73 and of W is 74. We therefore expect the two target surfaces to have similar photon yields. We estimate the photon yield of a Ta wire mesh to be

$$\bar{Y} = \frac{1}{2}\pi Y(0),$$

where  $Y(0)$  is the photon yield for normal incidence on a flat surface. In the estimate, we assume that the angular dependence of the photon yield has a  $\csc \theta$  dependence. Using the observed value for Ta at  $\theta = 0$ ,  $Y(0) = 3.96 \times 10^{-3}$  photon/sec, we find that  $\bar{Y} \approx 6 \times 10^{-3}$  photon/proton at 10.5 keV. This value compares closely with that of  $5 \times 10^{-3}$  obtained by Dunn *et al.*<sup>1</sup> for a tungsten mesh (note that their proton energy is 2.5 keV). This value is, however, nearly an order of magnitude greater than that reported by McCracken *et al.*<sup>5</sup> for 20-keV protons.

Shekhter<sup>17</sup> has considered a radiative process in which an ion near a metal surface is neutralized through a resonant electron transfer leading to the emission of a photon, rather than ejection of a second electron from the metal surface. The accessible states must lie below the Fermi energy,<sup>18</sup> i.e.,  $(E'_i - E'_x) > \phi$ , where  $E'_i - E'_x$  is the excited level relative to the continuum, and  $\phi$  is the work function. While this inequality holds for the process involving  $\text{He}^+$  described by Shekhter, it is invalid for populating  $H(2p)$  when protons are incident on molybdenum. Therefore, it is inappropriate to compare  $L_{\alpha}$  yields with Shekhter's calculation, as some investigators have done.<sup>1,2</sup>

### C. Line shape and energy dependence of the photon yield

From the line profile of the  $L_{\alpha}$  emission we observe both a blue shift and a less intense red-shifted component, as seen in Fig. 3. As pointed out by McCracken *et al.*, the blue shift is due to the Doppler shift of the emission of fast backscattered particles approaching the detector, and the red-shifted component can be explained as that from the reflection of the red-shifted radiation from the target surface. In our measurements, the Doppler shift is uncertain to  $\pm 0.5 \text{ \AA}$ .

The  $L_{\alpha}$  photon yield from a surface has a two-fold dependence on the incident proton energy. According to the simple Rutherford scattering formula, we see that the scattering cross sec-

tion is inversely proportional to the square of the particle energy at the instant of collision. On the other hand, the survival rate of an excited H atom as it leaves the surface has an exponential dependence of the form<sup>19</sup>

$$\exp(-A/av_n)$$

where  $A/a$  is a constant which characterizes the particle surface interaction, and  $v_n$  is the component of the velocity normal to the surface. The combined effects of these two factors provide an explanation for the energy dependence of the  $L_\alpha$  emission, and for the observed Doppler line shapes.<sup>4-9</sup>

#### D. Dependence of $L_\alpha$ photon yield on incident angle

The dependence of the  $L_\alpha$  emission on the angle of incidence can be qualitatively explained by the behavior of the backscattering proton flux. Oen and Robinson<sup>20</sup> have studied the reflection of H ions from amorphous Al, Cu, Nb, and Au. Using a binary-collision cascade-simulation program, they were able to make a theoretical calculation of the particle reflection from the surface as a function of particle incident angle. Their resulting reflection coefficients exhibit an angular dependence very similar to that which we observe for the  $L_\alpha$  photon yield. Baird, Zivitz, and Thomas<sup>6</sup> also report a similar angular dependence of the photon yield for Balmer- $\alpha$  emission from a Nb surface bombarded by protons.

A model which will predict the dependence of the  $L_\alpha$  photon yield on the incident particle energy and the incident angle has recently been developed.<sup>21</sup> Our treatment is similar to that of Olander *et al.*<sup>9</sup> in their calculation of Balmer line shapes, but employs a screened potential. The treatment also considers attenuation of the primary incident particle beam flux as it penetrates the solid surface. The results will be the subject of a later paper.

#### E. Temperature dependence

The observed temperature dependence of the photon yield is difficult to explain with existing theory. Note in Fig. 7 that the results for Ta and Mo surfaces exhibit a positive dependence. Single-crystal Si and Ge exhibit no temperature dependence in the range studied. The temperature dependence of the yield may be related to surface cleanliness. Rausch, Murray, Inouye, and Thomas<sup>22</sup> have studied the  $H_\beta$  line intensity from the bombardment of protons on Mo and Cu surfaces under different oxygen background pressures. They found that the  $H_\beta$  line intensity increases with the  $O_2$  pressure, and suggest that the change of intensity is caused by an increase of the survival rate of excited H atoms with the degree of cover-

age. In the case of a Cu surface, the observed temperature dependence of the yield suggests that at higher temperatures where the surface becomes cleaner, the excited H atom has a lower probability of survival. On the other hand, oxygen contamination of the Ge and Si surfaces is probably not effectively removed under the temperature range studied here.<sup>23</sup> The temperature behavior of the yield for Ta and Mo surfaces cannot be explained in the same manner.

Snouse and Bader<sup>24</sup> have found that sputtering yields from polycrystalline copper during 3-keV  $N_2^+$  bombardment show a marked decrease as the temperature increases. Carlston *et al.*<sup>25</sup> studied the sputtering yield of various types of crystal structures and reported that the temperature dependence of the sputtering yield is characteristic of the type of crystal bombarded. In the two polycrystalline fcc samples studied (Cu and Al), they found that the yield was approximately independent of temperature in the range 350–1000 °K for 2-, 5-, and 10-keV  $Ar^+$  bombardment, while for the polycrystalline bcc metals, Mo, W, and Ta, the sputtering yield increases linearly with temperature by 26%, 28%, and 39%, respectively. If the backscattering proton flux has the same temperature dependence as the sputtering yield, then the photon yield will be influenced by the effects of desorption on the one hand and by the temperature dependence of the backscattering flux on the other. Unfortunately, there are not many studies of the temperature dependence of backscattering reported.

#### F. Influence of absorbed hydrogen

It is of interest to investigate the possibility that the high photon yields may be due to proton-hydrogen interactions from a layer of hydrogen contaminating the target surface, as Dunn *et al.* suggested in 1960. We have increased our hydrogen background pressure from  $5 \times 10^{-9}$  to  $1 \times 10^{-7}$  Torr, with no noticeable increase of  $L_\alpha$  emission. Also, Khan *et al.*<sup>3</sup> have shown that the characteristic emission from particles already trapped in the crystal is negligibly small. From studies of field emission, Müller<sup>26</sup> and Gomer and Wortman<sup>27</sup> have observed that the desorption of adsorbed hydrogen from a W surface at high vacuum is virtually complete at about 600 and 700 °K, respectively. Pasternak and Wiesendanger,<sup>28</sup> in their studies of adsorption and desorption of hydrogen on molybdenum, reported a temperature dependence similar to that observed by Müller and by Gomer and Wortman. If the major contribution of the  $L_\alpha$  emission comes from proton-hydrogen interactions on the surface, we might expect a strong temperature dependence of the photon yield. The yield

should decrease with increasing target temperature; however, except for the case of a Cu surface, we do not see such a dependence. On the other hand, if we consider the interaction of the proton with an adsorbed hydrogen atom to be approximately the same as with a free H atom, we conclude that the contribution from this process will be within an order of magnitude of the observed yield if there is an H atom adsorbed for

every Cu atom. Thus, the contribution of  $H^+ + H$  interactions cannot be ruled out entirely. Conclusions by Sterk *et al.*<sup>1</sup> limit this contribution to no more than ~40%.

#### ACKNOWLEDGMENT

The authors wish to acknowledge many valuable discussions with B. Van Zyl.

- 
- <sup>1</sup>G. H. Dunn, R. Geballe, and D. Pretzer, *Phys. Rev.* **128**, 2200 (1962).  
<sup>2</sup>A. A. Sterk, C. L. Mark, and W. P. Saylor, *Phys. Rev. Lett.* **17**, 1037 (1966).  
<sup>3</sup>J. M. Kahn, D. L. Potter, R. D. Worley, S. I. Salem, and Harold P. Smith, Jr., *Phys. Rev. Lett.* **19**, 950 (1967).  
<sup>4</sup>G. M. McCracken and S. K. Erents, *Phys. Lett.* **31A**, 429 (1970).  
<sup>5</sup>G. M. McCracken and S. K. Erents (private communication); see also G. M. McCracken, *Rep. Prog. Phys.* **38**, 241 (1975).  
<sup>6</sup>W. E. Baird, M. Zivitz, and E. W. Thomas, *Phys. Rev. A* **12**, 876 (1975); *Nucl. Instrum. Methods* **132**, 445 (1976).  
<sup>7</sup>C. Kerkdijk and E. W. Thomas, *Physica* **63**, 557 (1973).  
<sup>8</sup>E. O. Rausch and E. W. Thomas, *Phys. Rev. A* **14**, 1912 (1976).  
<sup>9</sup>D. K. Olander, C. B. Kerkdijk, and C. Smith, *Surf. Sci.* **49**, 28 (1975).  
<sup>10</sup>C. D. Moak, H. Reese, Jr., and W. M. Good, *Nucleonics* **9**, 18 (1951).  
<sup>11</sup>M. J. Mumma and E. C. Zipf, *J. Chem. Phys.* **55**, 1661 (1971).  
<sup>12</sup>D. A. Vroom and F. J. DeHeer, *J. Chem. Phys.* **50**, 580 (1969).  
<sup>13</sup>E. J. Stone and E. C. Zipf, *J. Chem. Phys.* **56**, 4646 (1972).  
<sup>14</sup>J. W. McConkey and F. G. Donaldson, *Can. J. Phys.* **50**, 2211 (1972).  
<sup>15</sup>E. G. Schneider, *Phys. Rev.* **49**, 341 (1936).  
<sup>16</sup>A. H. Laufer, J. A. Piroy, and J. R. McNesby, *J. Opt. Soc. Am.* **55**, 65 (1965); D. F. Heath and P. A. Sacher, *Appl. Opt.* **5**, 937 (1966).  
<sup>17</sup>S. S. Shekhter, *Zh. Eksp. Teor. Phys.* **7**, 750 (1937).  
<sup>18</sup>H. D. Hagstrum, *Phys. Rev.* **96**, 336 (1954).  
<sup>19</sup>W. F. Van der Weg and D. J. Bierman, *Physica* **44**, 206 (1969).  
<sup>20</sup>O. S. Oen and M. T. Robinson, *Nucl. Instrum. Methods* **132**, 647 (1976).  
<sup>21</sup>Y.-Y. R. Hsiao, thesis (University of Denver, 1977) (unpublished).  
<sup>22</sup>E. O. Rausch, M. W. Murray, H. Inouye, and E. W. Thomas, *J. Appl. Phys.* **48**, 4347 (1977).  
<sup>23</sup>B. A. Joyce, *Surf. Sci.* **35**, 1 (1973).  
<sup>24</sup>T. W. Snouse and M. Bader, *Transactions of the Eighth National Vacuum Symposium, Washington, 1961* (Perгамon, New York, 1962), Vol. 1, p. 271.  
<sup>25</sup>C. E. Carlston, G. D. Magnuson, A. Comeaux, and P. Mahadevan, *Phys. Rev.* **138**, A759 (1965).  
<sup>26</sup>E. W. Müller, *Ergeb. Exakten. Naturwiss.* **27**, 290 (1953).  
<sup>27</sup>R. Gomer and E. R. Wortman, *J. Chem. Phys.* **23**, 1741 (1955).  
<sup>28</sup>R. A. Pasternak and Hans U. D. Wiesendanger, *J. Chem. Phys.* **34**, 2062 (1960).